

DEMANDS ON TURBULENCE MODELLING FOR VENTILATED ROOM AIRFLOWS

Christian HESCHL^{1*}, Wolfgang SANZ² and Ines LINDMEIER¹

¹ University of Applied Science, Burgenland, Pinkafeld 7423, AUSTRIA

² Institute for Thermal Turbomachinery and Machine Dynamics, University of Technology, Graz 8010, AUSTRIA

*Corresponding author, E-mail address: Christian.Heschl@fh-burgenland.at

ABSTRACT

In buildings very exact thermal conditions are often needed to ensure a high quality production process or comfortable indoor environment. To fulfil these requirements the accurate prediction of room airflows plays an important part in the design process of ventilation systems. Computational Fluid Dynamics (CFD) is a promising tool in this context. But a reliable CFD prediction implies a correct description of the turbulence quantities. For this reason complex three-dimensional room airflow situations were investigated with Particle Image Velocimetry to get detailed information about the flow topology, the Reynolds-stress distribution and the entrainment. Based on the experimental results the demand on RANS-based turbulence models for predicting room airflows will be discussed. In this context it will be shown that intensive anisotropic Reynolds-stresses near the wall and transitional effects in the inlet region (Reynolds number influence on jet spreading rate) influence the airflow pattern. Based on the experimental findings an algebraic Reynolds-stress turbulence model will be proposed. Compared with other linear eddy viscosity and Reynolds stress models this nonlinear model agrees clearly better with the presented experimental findings.

NOMENCLATURE

b_{ij}	Reynolds stress anisotropy tensor [1]
$b_{ij} = (\overline{u'_i u'_i} - 2/3 k \delta_{ij}) / 2k$	
k	kinetic turbulence energy [m^2/s^2]
S_{ij}	strain rate tensor [1/s]
T	turbulent time scale [s]
u_i	time averaged velocity [m/s]
$\overline{u'_i u'_i}$	Reynolds stress tensor [m^2/s^2]
NL	nonlinear modification presented in this paper
KW	standard k- ω turbulence model*
KW-PENG	k- ω turbulence model by Peng (1998)
KW-SFC	k- ω model with shear flow correction*
RKE	realizable turbulence model by Shih et al. (1995)*
RSM-IP	Reynolds stress model by Gibson and Launder (1978)*
SKE	Standard k- ε turbulence model*

*Standard model setup according to Fluent (2007).

ε	dissipation rate [m^2/s^3]
η	non-dimensional invariant [1]
ζ	non-dimensional invariant [1]
Ω_{ij}	rotation rate tensor [1/s]

INTRODUCTION

Due to the lower computational effort most airflow simulations are based on the Reynolds Averaged Navier Stokes equations (RANS) with a first-order-closure turbulence model. Generally most models use a linear correlation between the Reynolds stress tensor and the strain rate tensor. But it is generally known that the default Boussinesq approach is not able to suitably reproduce the turbulent normal stresses. For this reason the approach fails e.g. in the area of stagnation points (Kato et al., 1993) and in the prediction of turbulence-driven secondary motions (Demuren et al., 1984). Within room airflows both flow situations can be observed. The first flow situation is e.g. present in production facilities when the airflow is used for cooling the machinery. The second flow situation exists when the air inlet is mounted near a wall so that a three-dimensional wall jet can arise. In that case the redistribution of the turbulent normal stresses near the wall produces a remarkable motion of the jet in lateral direction so that the global flow pattern will be changed (Abrahamsson, 1997; Craft et al., 2001 and Lübcke et al., 2003).

Besides the influence of the turbulent normal stresses another effect must be considered carefully. Commonly in ventilated rooms the air inlet velocity is low so that the Reynolds number is in a range of $\text{Re} = \sim 10^2 \dots \sim 10^4$. In this range transitional effects which alter the entrainment of the inlet jet are present and the jet spreading rate depends on the Re number (Regenscheit, 1976; Hanel et al., 1979; Deo 2005 and Deo et al., 2007). Current turbulence models are not able to consider such transitional effects, so that an accurate computation of room airflows still requires specific model modifications.

The importance of the turbulent normal stresses and the transitional effects indicates that a nonlinear eddy-viscosity turbulence model (EVM) with a specific calibration with regard to normal stresses and entrainment can better predict room airflows. Therefore in this paper a nonlinear EVM modification which can be simply calibrated will be presented. Furthermore own experimental findings about turbulent normal stress distribution, entrainment and global airflow pattern for ventilated rooms will be shown. Based on the experimental data the potential of the specifically calibrated

nonlinear eddy viscosity turbulence model will be discussed.

MODEL DESCRIPTION

Nonlinear Eddy Viscosity Modification

In principle nonlinear eddy viscosity models assume that the anisotropy tensor depends on the local velocity gradients and the turbulent time scale. For two-dimensional flows only three linear independent tensor components are sufficient to reproduce anisotropy of turbulent normal stresses (Gatski et al., 1992) so that the Reynolds stress anisotropy tensor can be determined as follows:

$$b_{ij} = -C_\mu T S_{ij} - C_\mu C_1 T^2 \left(S_{ik} S_{kj} - \frac{1}{3} S_{kl} S_{kl} \delta_{ij} \right) - C_\mu C_2 T^2 \left(\Omega_{ik} S_{kj} - \Omega_{jk} S_{ki} \right) \quad (1)$$

For simple shear flows the coefficients C_1 and C_2 can be determined directly from experimental and DNS data. For example some appropriate investigations are summarized in Table 1.

author	η	ξ	b_{11}	b_{22}
Kim et al. (1987)	3.30	3.30	0.179	-0.127
Tavoularis et al. (1989)	4.30	4.30	0.220	-0.160
Tavoularis et al. (1981)	6.08	6.08	0.202	-0.145
Tavoularis et al. (1981)	6.25	6.25	0.200	-0.150
de Souza et al. (1995)	7.70	7.70	0.180	-0.110
Laufer (1951)	3.10	3.10	0.220	-0.150

Table 1: Anisotropy tensor for different shear flows.

These results indicate that an accurate determination of the anisotropy tensor b_{ij} requires variable coefficients. For homogeneous shear and boundary layer flows the anisotropy tensor b_{12} is proportional to the non-dimensional invariants

$$\eta = T \sqrt{2S_{ij}S_{ij}} \quad \text{and} \quad \xi = T \sqrt{2\Omega_{ij}\Omega_{ij}} \quad (2)$$

and b_{ii} is proportional to η^2 and ξ^2 , so that the following approach is suggested:

$$C_i = C_i(\gamma^2) \quad \text{and} \quad \gamma = \sqrt{0.5(\eta^2 + \xi^2)} \quad (3)$$

Based on the results summarized in Table 1 and on equation (3) the following approximation is suggested:

$$C_1 = C_2 = \frac{-1.9}{0.9 + \gamma^2} \quad \text{with} \quad C_\mu = 0.09 \quad (4)$$

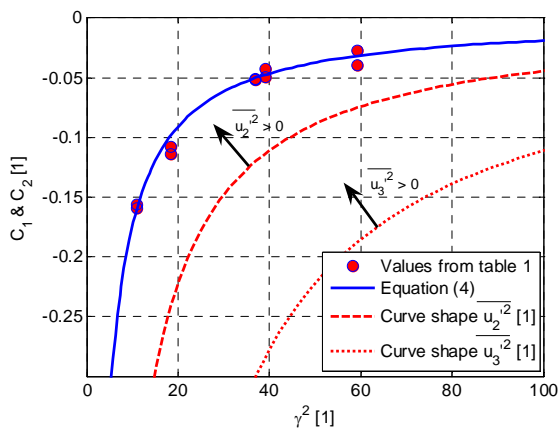


Figure 1: Characteristics of the coefficients C_1 and C_2 .

Fig. 1 shows the dependence of the model coefficients C_1 and C_2 on the invariant parameter γ . Additionally, for simple shear flows the ranges with positive normal stresses, are also indicated. The curve shapes demonstrate that equation (4) ensures positive turbulent normal stresses so that compared to conventional nonlinear eddy viscosity models a better numerical robustness can be expected.

Calibration of Entrainment

Motivation

In ventilated rooms usually low inlet velocities are used to avoid draught risk in occupied zone. Therefore low Reynolds jets are often used in the inlet area. This has a far-reaching consequence. It is well known that the spreading rate of free jets between $Re = \sim 10^2 \dots \sim 10^4$ depends on the Reynolds number. Turbulence models are not able to reproduce such transitional effects. For example, the experimental investigation of the Reynolds number influence on jet spreading rate (transitional behaviour) by Deo (2005) is evaluated. Deo's inlet geometry and the used computational domain are shown in Fig. 2.

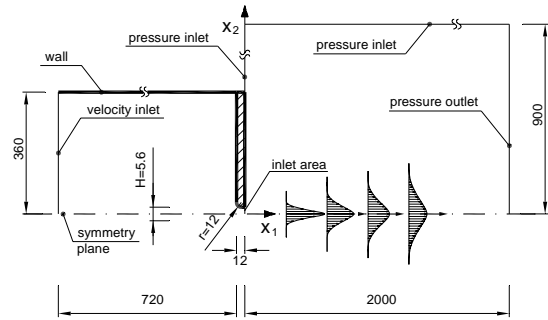


Figure 2: Measurement setup of Deo (2005) and derived computational domain (dimensions in mm).

To illustrate the restriction of RANS based turbulence models, in Fig. 3 the development of the spreading rate in dependence of the Reynolds number is represented. The measured spreading rate clearly increases with decreasing Reynolds numbers. By contrast, all used turbulence models predict different and nearly constant spreading rates. The range of the different computed spreading rates is almost in the band of the measured data. E.g. the best choice for low Reynolds number jets are the RSM-IP, KW and SKE models and for high Reynolds number jets the V2F, KW-SFC and RKE models.

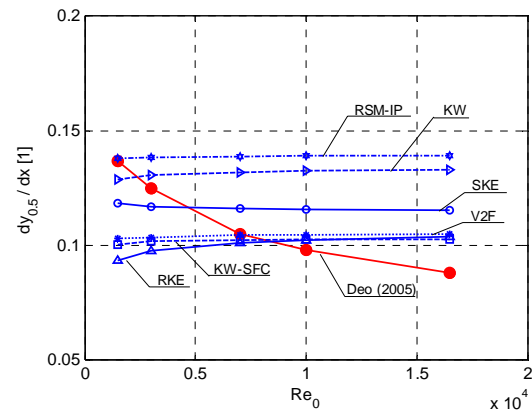


Figure 3: Spreading rates computed with different turbulence models.

Since at the time no turbulence model for a RANS solution of this transitional behaviour of free jets exists, an individual adjustment of the model constants is necessary to reproduce the different spreading rates.

Proposal of a simple calibration procedure for standard eddy viscosity models

An individual tuning of model constants should be consistent to the log-law layer. A detailed discussion about the log-law layer behaviour and the interdependence of the model constants can be found in Durbin and Pettersson Reif (2001) and Wilcox (2005). According to that a simple option is to adapt the proportionality factor of the production and dissipation term in the ϵ or ω equation in such a way that the spreading rate and the logarithmic wall law are fulfilled. According to k- ϵ and k- ω based turbulence models the following link between the model parameters should be ensured:

$$\kappa^2 = (C_{\epsilon 2} - C_{\epsilon 1}) \sigma_{\epsilon} \sqrt{C_{\mu}} \quad (5)$$

$$\alpha_{\infty} = \frac{\beta}{\beta_{\infty}^*} - \frac{\kappa^2}{\sigma_{\omega} \sqrt{\beta_{\infty}^*}} \quad (6)$$

If the spreading rate is known, a specific calibration of the model constants based on the equation (5) and (6) is feasible. The necessary experimental effort is only the measurement of the mean inlet velocity and the spreading rate. The investigation of the statistic moments of second order (e.g. the Reynolds stresses) is not necessary.

MEASUREMENT SETUP

Test rig

The test rig for the experimental investigations consists of an air supply system with a mass flow meter, a model room made of plexiglass in an air-conditioned test room and a PIV (Particle Image Velocimetry) measurement system. The PIV system is used for two and three dimensional measurements. The experimental arrangement is shown in Fig. 4. The test rig is equipped with a frequency-controlled fan unit, which feeds the air via an orifice plate, rectifier, flow measurement unit, temperature sensors and seeding mixing chamber to the

plexiglass test model. To get a better illumination the plexiglass model is set inside a black coated test room. In order to minimize the thermal influences the laser energy supply and the computer equipment are placed outside of the test room. To ensure isothermal conditions the test room is additionally ventilated. The inlet air temperature, the outlet air temperature and the surface temperature of the surrounding walls of the plexiglass model are continuously monitored by 10 Pt100 temperature sensors. Also the ambient pressure and the inlet mass flow are monitored. The light sheet optics and the two cameras are mounted on a two dimensional traverse system, so that only one calibration for the PIV measurements has to be done.

During the measurement the temperatures, the relative humidity and the ambient pressure are logged, so that the air properties can be determined. The measurement planes are chosen in such a way that the whole flow area in a x-y plane (see Figs. 5 and 6) can be measured by moving the lightsheet and camera with the traverse system. A detailed description of the used PIV setup (interrogation areas, overlapping, correlation method etc.) is given by Heschl et al. (2008).

Scale models

The dimensions of the two plexiglass models investigated are shown in Figs. 5 and 6. The plexiglass models differ by different length-to-height and length-to-width ratios and by different outlet openings. Both models have an air supply duct (38 x 3mm) with evenly distributed holes. Both supply ducts are fed from both end sides over a flow rectifier.

The air supply duct of the first model has 222 holes with a diameter of 2 mm and a distance between the holes of 3 mm. The overall inlet and outlet length is 666 mm. The mean inlet velocity is 14.84 m/s and the inlet angle is 16° measured to the horizontal direction. The air leaves the model through a small channel at the opposite side.

The air supply duct of the second model has 7 groups of 32 holes with a diameter of 1.3 mm and an overall length of 440.8 mm. The distance between the holes is 1.5 mm and between the seven-hole groups 13.5 mm. The mean inlet velocity is 36.88 m/s and the inlet angle is 27.5° measured to the horizontal direction.

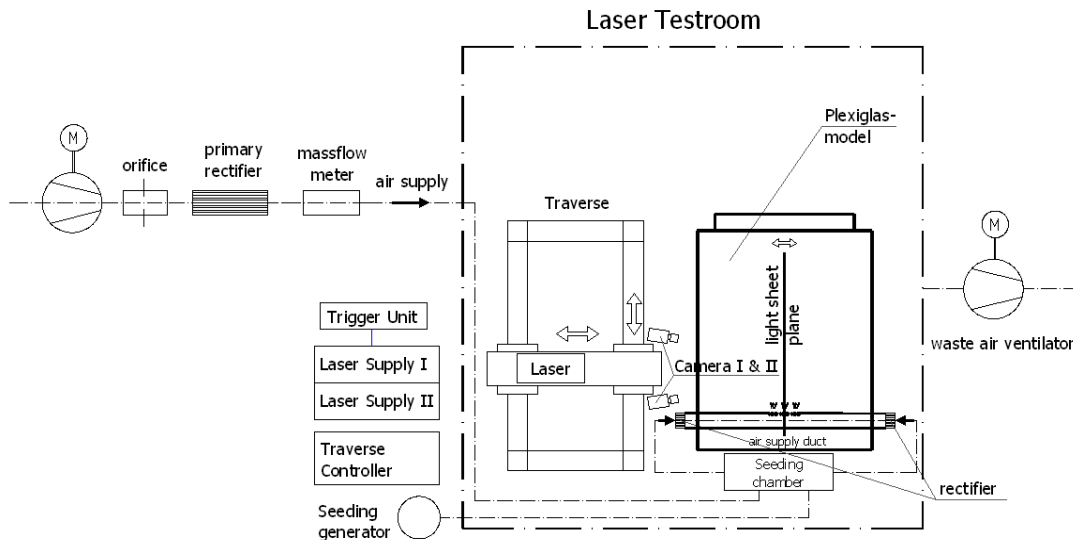


Figure 4: Measurement arrangement for the experimental investigation.

The outlet duct is identically equal to the air supply duct - but the holes are arranged on the bottom side.

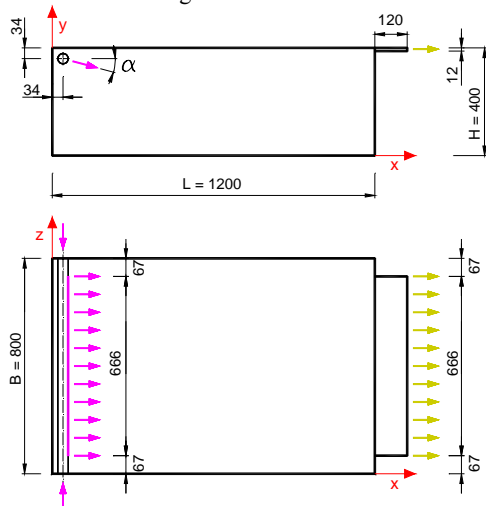


Figure 5: Geometry of the plexiglass model room I (dimensions in mm)

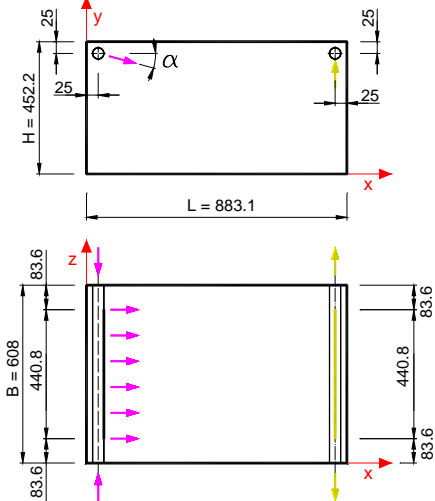


Figure 6: Geometry of the plexiglass model room II (dimensions in mm)

For the second model the arrangement of the supply holes is shown in detail in Fig. 7.

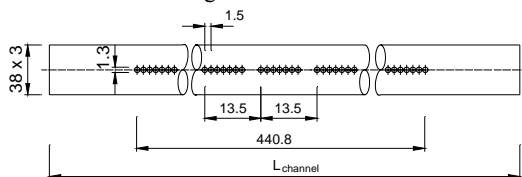


Figure 7: Principle geometry of the air supply duct for the plexiglass model room II

All measurements are done at isothermal boundary conditions.

VALIDATION RESULTS

Numerical Setup

In all test cases a geometrical inlet simplification was used. Instead of a detailed resolution of the inlet holes a slot with the same outlet area was considered.

The computational results are obtained with the commercial CFD code Fluent 6.3.26 (Fluent, 2007). The

SIMPLE based segregated solver is used, for the convective terms the second order upwind discretization is applied.

Beside the standard turbulence models (SKE, RKE, KW-SFC and RSM-IP) the KW-PENG model - which was designed especially for room airflow prediction - was used. Furthermore the proposed nonlinear eddy viscosity modification was applied to the SKE and KW-PENG model leading to the SKE-NL und KW-PENG-NL model. The implementation in Fluent was done with UDF-routines. The required turbulent time scale was determined from equation (7).

$$T = \frac{k}{\varepsilon} \quad T = \frac{\alpha^*}{C_\mu \omega} \quad (7)$$

Additionally, the calibration procedure for the entrainment process as described above was applied to the nonlinear versions. Hence a separate experimental setup was used to measure the spreading rate for the two investigated inlet ducts. For the air supply duct of model room I a spreading rate of $dy_{1/2}/dx=0.110$ and of model room II of $dy_{1/2}/dx=0.108$ were determined. The proposed calibration procedure (equation (5) and (6)) yield to $C_{\varepsilon 1}=1.42$, $\sigma_\varepsilon=1.23$ for the SKE-NL and $\alpha_\omega=0.40$, $\sigma_\omega=1.30$ for the KW-PENG-NL, respectively. The other model constants conform to the standard values. All used turbulence models show good convergence behaviour.

For both model rooms two different grids – a fine and a coarse grid – are used. The coarse grid was designed with a $y^+ \sim 30$ for turbulence models with standard wall functions (SKE, SKE-NL, RKE and RSM-IP models). The number of grid cells for the whole computational domain is about 1.200.000 for model room I and 2.500.000 for model room II. The fine grid was designed for near-wall low-Re turbulence models (KW-PENG, KW-PENG-NL and KW-SFC models) with a $y^+ < 1$. The number of grid cells for the computational domain is about 3.500.000 for model room I and 2.500.000 for model room II.

Computation and measurement results

The measured (top row) and predicted (remaining row) velocity distribution is shown in Fig. 8 and Fig. 10 for model room I and II. In both cases the flow contains a free jet in the inlet region and downstream a wall affected area. In this area the flow is driven by the Coanda effect which presses the jet towards the ceiling. The measurement results of model room I point out that a nearly symmetrical room airflow arises. By contrast, in model room II the room airflow is clearly asymmetrical. This principal flow behaviour is reproduced by all used turbulence models. Only the KW-SFC and partly the RKE model predict asymmetrical airflow in model room I. Both models determine the turbulence interaction too dissipative so that the entrainment is significantly underpredicted (the measured spreading rate in the inlet area is about $dy_{1/2}/dx=0.11$ and the predicted $dy_{1/2}/dx=0.09$). This leads to a lower entrainment in the shear layer flow and consequently to a too small jet profile with a too high centreline velocity and to an unsteady flow condition - although steady state airflow behaviour was measured. This behaviour of the RKE and KW-SFC model can also be observed in model room II. Both models predict too little entrainment so that a complete attachment of the jet to the wall is suppressed. In contrast, the simple SKE model with a computed spreading rate of

$dy_{1/2}/dx=0.11$ predicts the flow pattern and the velocity distribution clearly better than the RKE, KW-SFC and RSM-IP model.

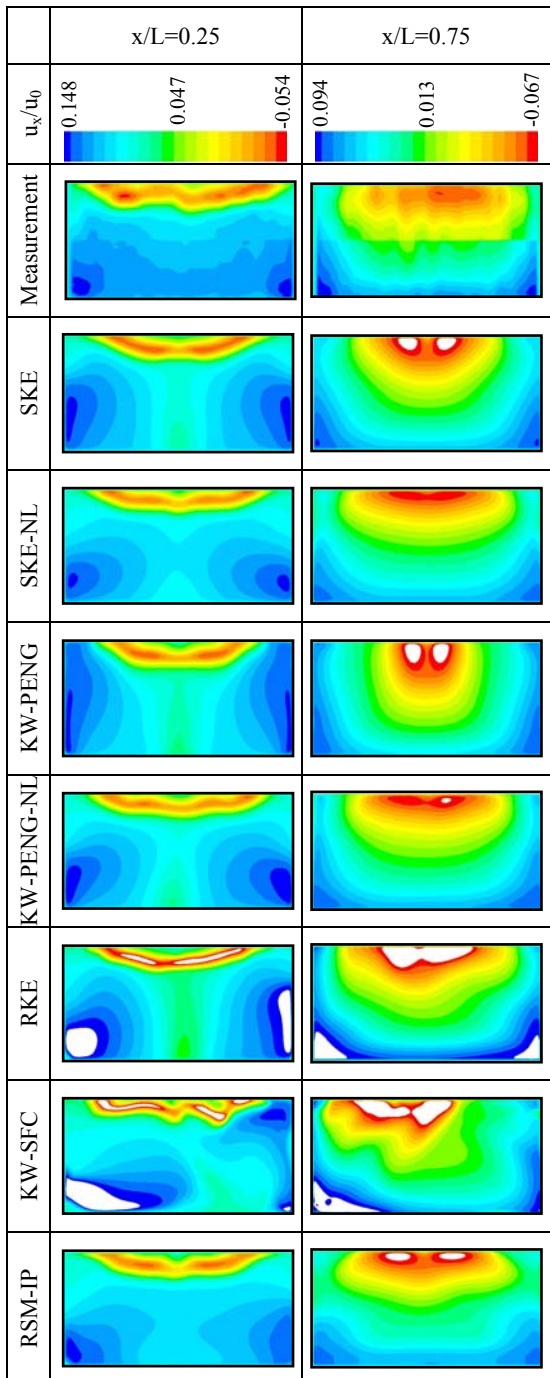


Figure 8: Comparison of measured and computed velocity distribution in model room I

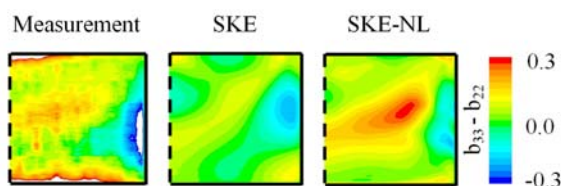


Figure 9: Measured and computed anisotropy tensor difference $b_{33}-b_{22}$ in the $x=L/2$ plane of the model room I

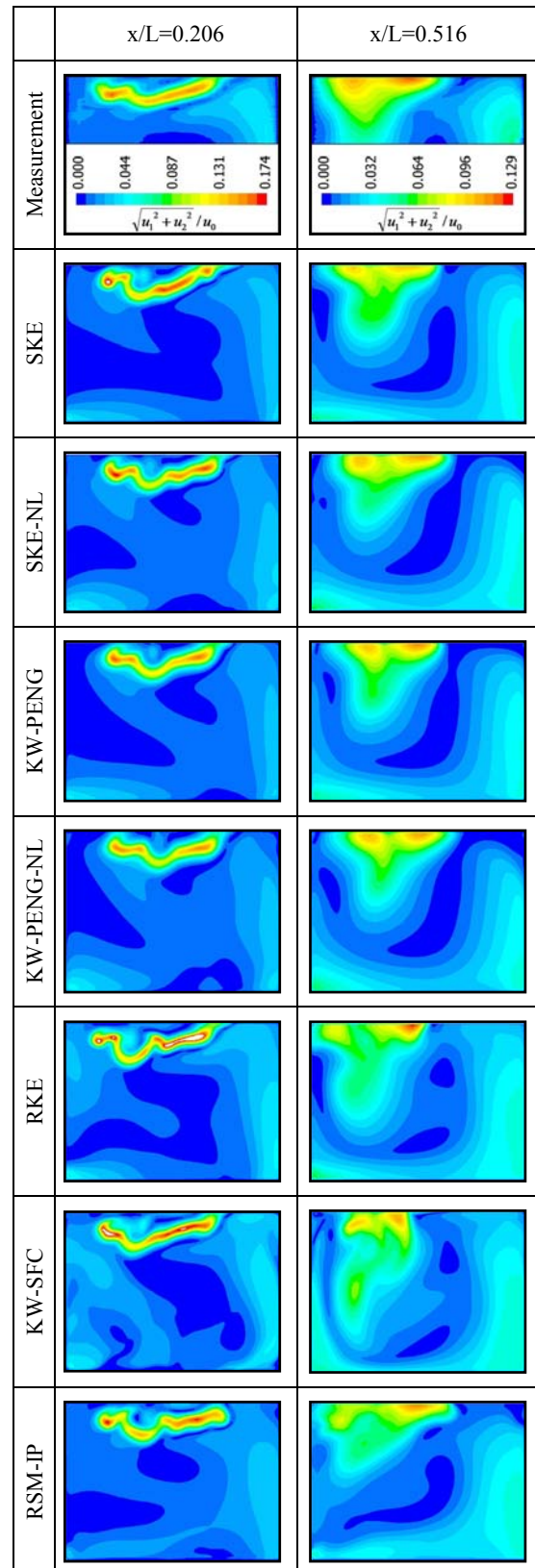


Figure 10: Comparison of measured and computed velocity distribution in model room II

The computed flow pattern indicates that an accurate prediction of the entrainment is very important. Because of the low inlet velocity a transitional flow behaviour - which leads to a higher entrainment effect (see Fig. 3) - can be expected. Consequently turbulence models which

are calibrated for high Reynolds free shear layer flows are not able to reproduce the velocity distribution. Accordingly the model constants of RANS-based turbulence models should be adjusted before they will be used for room airflow simulations.

The impact of the nonlinear correlation between the anisotropy and the strain rate and rotation rate tensor can be analysed from Fig. 8 and 10. The comparison of the velocity distribution between the SKE and the SKE-NL model as well as the KW-PENG and the KW-PENG-NL model in Fig. 8 shows that the nonlinear models clearly better agree with the experimental findings. Especially far away from the inlet ($x/L=0.75$) the flow pattern of the wall jet at the ceiling is more realistically reproduced. The improved normal stress distribution of the nonlinear model (see Fig. 9) enables the turbulence driven secondary motion which improves the prediction of the lateral spreading rate of the three dimensional wall jet on the ceiling. In comparison with the differential Reynolds stress model (RSM-IP) the nonlinear eddy viscosity model gives comparable results but needs less computational effort.

Interestingly, the remarkable influence of the turbulent normal stresses can not be noticed in model room II (see Fig. 10). Due to the larger inlet angle and the smaller room length only a poorly distinct wall jet arises so that the effect of the normal stresses are negligible.

CONCLUSION

In industrial applications RANS based turbulence models are widely used. But generally they are not able to predict transitional effects, i.e. the growing spreading rate of wall jets with lower Reynolds number. Especially at room airflows often low inlet velocities are given so that a detailed investigation of the transitional effect on the airflow pattern is necessary. For this reason a simple calibration procedure for eddy viscosity turbulence models which ensure the log-law and shear-layer behaviour is presented. In addition a nonlinear eddy viscosity model is suggested to reproduce the anisotropic Reynolds stresses and consequently turbulence driven secondary motions. Finally both approaches are validated with own experimental findings of two different complex room airflows. Thereby it could be shown that the suggested approaches improve significantly the predicted velocity distribution in ventilated rooms.

ACKNOWLEDGEMENT

The investigations were partly accomplished by the FFG structure program Josef Ressel-Zentrum "CFD-Centre Austria".

REFERENCES

ABRAHAMSSON, H., (1997), "On Turbulent Wall Jets", *PhD thesis*, Department of Thermo and Fluid Dynamics, Chalmers University of Technology, Göteborg Sweden. ISBN 91-7197-491-1.

CRAFT, T.J., LAUNDER, B.E., (2001), "On the spreading mechanism of the three-dimensional turbulent wall jet", *Journal of Fluid Mechanics*, Vol. 435: Pages 305-326.

DE SOUZA, F.A. NGUYEN, D. and TAVOULARIS, S. (1995), "The structure of highly sheared turbulence", *Journal of Fluid Mechanics*, Vol. 303.

DEMUREN, A.O. and RODI, W. (1984), "Calculation of turbulence-driven secondary motion in non-circular ducts", *Journal of Fluid Mechanics*, Vol. 140.

DEO R. C. (2005), "Experimental Investigations of the Influence of Reynolds Number and Boundary Conditions on a Plane Air Jet", *PhD-Thesis*, University of Adelaide, South Australia

DEO, C., MI, J. and NATHAN G., J., (2007), "Experimental Investigations of the Effect of Reynolds Number on a Plane Jet", 16th *Australian Fluid Mechanics Conference*, Crown Plaza, Gold Coast.

DURBIN, P.A., PETERSSON REIF, B.A., (2001), "Statistical Theory and Modeling for Turbulent Flows", *John Wiley & Sons, Ltd*, New York – Weinheim – Brisbane – Singapore – Toronto, ISBN 0 471 49736 3.

FLUENT (2007), "FLUENT 12 User's Guide", *Fluent Inc. Centerra Resource Park*, Lebanon.

GATSKI, T.B. and SPEZIALE, C.G. (1992), "On explicit algebraic stress models for complex turbulent flows", *Technical Report 92-58*, Institute for Computer Application in Science and Engineering.

GIBSON, M.M. and LAUNDER, B.E. (1978), "Ground Effects on Pressure Fluctuations in the Atmospheric Boundary Layer", *J. Fluid Mech.*: 86:491-511.

HANEL, B. and RICHTER, E., (1979), „Das Verhalten von Freistrahlen in verschiedenen Reynolds-Zahlenbereichen“, *Luft- und Kältetechnik*, Vol. 1

HESCHL, Ch., SANZ, W. and LINDMEIER, I. (2008)., „Experimental investigations of the turbulent mixing process and the Reynolds-stress anisotropy tensor in ventilated rooms“, *29th AIVC Conference*, Kyoto, Japan.

KATO, M.; LAUNDER, B.E., (1993), "The modelling of turbulent flow around stationary and vibrating cylinders", *Ninth Symposium on turbulent shear flows*, Kyoto, pp 10-4-1 10-4-6

KIM, J., MOIN, P. and MOSER, R. (1987), "Turbulence statistics in fully developed channel flow at low Reynolds number", *J. of Fluid Mechanics*, Vol. 177.

LAUFER, J. (1951)., "Investigation of turbulent flow in a two dimensional channel", *Tech. Rep. 1053, NACA*.

LÜBCKE, H.M., RUNG, Th., THIELE F. (2003), "Prediction of the spreading mechanism of 3D turbulent wall jets with explicit Reynolds-stress closure", *Int. Journal of Heat and Fluid Flow*, Vol. 24: Pages 434-443.

PENG S., (1998), "Modelling of Turbulent Flow and Heat Transfer for Building Ventilation", *PhD-Thesis*, Chalmers University of Technology, Gothenburg

REGENSCHEIT, B. (1976), "Einfluss der Reynoldszahl auf die Geschwindigkeitsabnahme turbulenter Freistrahlen", *Heizung Lüftung/Klima Haustechnik* 27, Vol. 4, pages 122-126

SHIH T.-H., LIOU W.W., SHABBIR A. and ZHUN J., (1995), "A New k-ε Eddy-Viscosity Model for High Reynolds Number Turbulent Flows – Model Development and Validation", *Computers Fluids*, Vol. 24

TAVOULARIS, S. and CORRISIN, A. (1981), "Experiments in Nearly Homogeneous Turbulent Shear Flow with a Uniform Mean Temperature Gradient Part I", *J. Fluid Mech.* Vol. 104: pp. 311-347.

TAVOULARIS, S. and KARNIK U. (1989), "Further experiments on the evolution of turbulent stresses and scales in uniformly sheared turbulence", *J. of Fluid mech.*, Vol. 204.

WILCOX, D.C., (2005), "Turbulence Modeling for CFD. Third Edition", *DCW Industries, Inc.*, ISBN 978-1-928729-08-2, USA San Diego.